

Experiments on the upstream wake in magneto-fluid dynamics

By HARLOW G. AHLSTROM

Graduate Aeronautical Laboratories, California Institute of Technology,
Pasadena, California

(Received 25 July 1962)

Measurements have been made of the perturbation magnetic field in front of a semi-infinite Rankine body, moving parallel to a uniform impressed magnetic field in a conducting fluid. The purpose of these experiments was to investigate the so-called upstream wake effect which has been predicted by theory. It is believed that these are the first experiments in which the upstream wake has been observed. Although the wake was found to exist as predicted when the Alfvén number is greater than one, its decay behaviour was remarkably different from that which was predicted. The solutions for an infinite medium predicted that in the wake the perturbations should decay inversely as the distance from the body. However, the experiments showed that the perturbations decayed exponentially. It was finally shown that this change in the decay behaviour was an effect of the walls and the conducting material surrounding the fluid.

1. Introduction

This paper presents the results of experiments on the flow of a conducting fluid, mercury, over a semi-infinite body in the presence of a parallel applied magnetic field. The general problem of the flow of a conducting fluid over a body in the presence of an applied magnetic field has been studied theoretically by many authors. Chester (1957) studied the sphere for low Reynolds numbers and low conductivity, Greenspan & Carrier (1959) studied the flow over a flat plate, Stewartson (1960) studied flows in which the conductivity is infinite, Van Blerkom (1960) and Gourdine (1961) have found fundamental solutions, and Lary (1962) and Tamada (1961) studied two-dimensional infinite-Reynolds-number flows. The most interesting result from these theoretical investigations was the prediction of the existence of an 'upstream wake' under certain conditions. The mechanism for the production of this new wake is the propagation of Alfvén waves which carry both vorticity and current. When the propagation speed is greater than the body speed, then wakes are formed both upstream and downstream of the body and when the propagation speed is less than the speed of the body, then wakes are formed in the downstream direction only.

The basic dimensionless parameters for this problem are:

Reynolds number $Re = UD/\nu \approx [(body\ speed)/(\text{viscous diffusion speed})]^2$,

Magnetic Reynolds number

$Rm = \sigma\mu UD \approx [(body\ speed)/(\text{magnetic diffusion speed})]^2$,

Alfvén number $\alpha = B_0/(\rho\mu)^{\frac{1}{2}}U \approx (\text{Alfvén wave speed})/(\text{body speed}),$

Magnetic Oseen number $k = \frac{1}{2}(1 - \alpha^2)Rm,$

where U is the speed of the body, B_0 is the uniform magnetic field strength, D is the body diameter, ρ is the mass density of the mercury, ν is the kinematic coefficient of viscosity, σ is the electrical conductivity and μ is the permeability with all units in the m.k.s.q. system. The magnetic Oseen number appears as the parameter in the Oseen-type equations for the electric current density, \mathbf{J} , and the vorticity, $\boldsymbol{\omega}$; in the limit $Re \rightarrow \infty$, these equations are $(\nabla^2 - 2k \partial/\partial z)\mathbf{J}$, $\boldsymbol{\omega} = 0$ (see Appendix). This parameter could more accurately be called a Reynolds number since it plays the same role as the ordinary Reynolds number in classical fluid dynamics. It is a combination of Rm , defined above, and $\alpha^2 Rm$ which is the ratio of the magnetic forces to the inertial forces. The magnetic force per unit volume is $(\mathbf{J} \times \mathbf{B}) = \sigma(\mathbf{V} \times \mathbf{B}) \times \mathbf{B}$, where \mathbf{V} is the fluid velocity; this gives the dimensional factor $\sigma U B_0^2 D^3$ for the magnetic force. Dividing by the dimensional factor for the inertial forces, $\rho U^2 D^2$, one obtains $\alpha^2 Rm$.

In order to investigate this upstream wake experimentally, the magnetic field perturbations were measured in the region forward of a semi-infinite body in the parallel magneto-fluid-dynamic flow.

2. Experiments

The experiments were performed in a facility which is called the mercury tow tank. This facility consists of a stainless steel tube of inner diameter $5\frac{1}{2}$ in. and 55 in. long filled with mercury. Surrounding the tube is a water-cooled solenoid which produced a uniform magnetic field of up to 8300 G in the axial direction in the tank (see figure 1). The facility receives its designation as a tow tank from the feature that the model is driven through the tank on the end of a 1 in. diameter sting at speeds up to 2 m per sec. The sting comes up through a seal in the bottom of the tank. Below the tank the sting is connected to a drive motor. The drive system is designed so that the model is accelerated very rapidly (5 to 10 g) to the desired speed and then runs at this speed until the experiment is completed, when a brake is applied to bring the model to rest. A complete description of the facility has been given by Liepmann, Hault & Ahlstrom (1962).

The model chosen for these experiments is a semi-infinite Rankine body, i.e. the body defined by a source in a uniform stream. There are several reasons for choosing this particular model. First, the model is just an extension of the sting so that the sting is part of the model, which is a natural and clean configuration. Secondly, if a closed body were used, the body would have to be mounted on a very thin sting which would extend from the end of the drive sting. This configuration would introduce two factors which would confuse the problem; these are the effect of the drive sting on the flow and the possible effect of separated flow on the body. Thirdly, for the semi-infinite Rankine body an analytical solution is known for the flow in the absence of magnetic effects.

In order to measure the magnetic field perturbations, 1000-turn pick-up coils are used. The pick-up coils have a larger diameter than the model and are mounted

stationary in the tow tank with their centres on the axis of symmetry (see figure 1). The model carries with it a distribution of magnetic field so that as the model approaches and passes through the pick-up coil, the coil senses a change in the magnetic field strength which induces a voltage that can be measured.

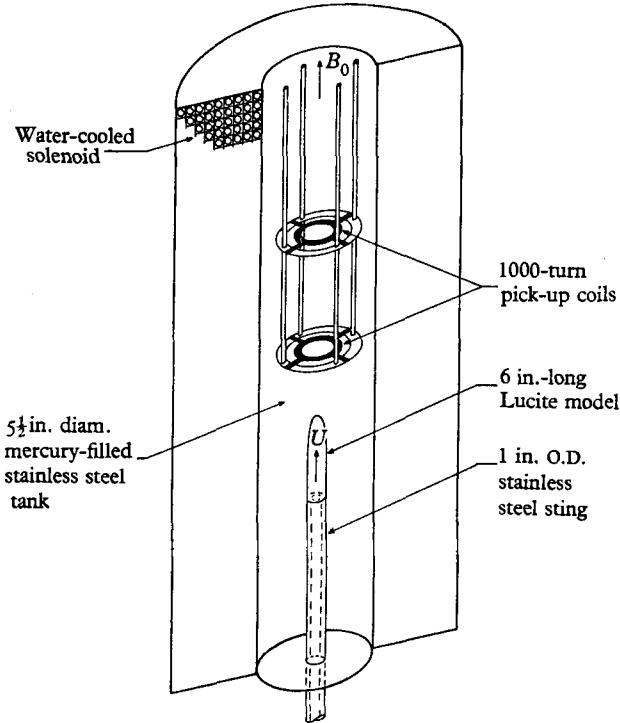


FIGURE 1. Mercury tow tank.

The voltage in the pick-up coil is

$$\oint \mathbf{E} \cdot d\mathbf{s} = -N \frac{\partial}{\partial t} \iint \mathbf{B} \cdot \mathbf{n} dA.$$

The voltage is integrated electronically so that a quantity

$$V \propto \int_{A_c} B_z dA,$$

is the recorded measurement. From the equation of continuity $\text{div } \mathbf{B} = 0$, V is also proportional to

$$\int_{-\infty}^z R_c B_R(R_c, z) dz$$

and to the magnetic stream function or magnetic flux, Ψ , defined by

$$B_z = \frac{1}{R} \frac{\partial \Psi}{\partial R}, \quad B_R = -\frac{1}{R} \frac{\partial \Psi}{\partial z}.$$

Here B_z and B_R are the axial and radial components of the magnetic field perturbations, R_c is the radius of the coil, A_c is the area enclosed by the coil and N

is the number of turns of the coil. Then since four coils with diameters of 1.16, 1.54, 1.94 and 2.34 in. were used, it is possible to determine average values of B_z and local values of B_R and Ψ as functions of z for four values of R .

For the actual measurements two identical coils are used, one mounted 6 in. above the other. The lower coil measures the signal and the noise; the upper coil measures the signal delayed a known amount and the noise. The two signals are subtracted by a d.c. differential amplifier, integrated, displayed on an oscilloscope, and recorded by a Polaroid camera. The signal recorded from the two coils is then

$$\int_{A_c} B_z(z) dA - \int_{A_c} B_z(z+6) dA,$$

where

$$\int_{A_c} B_z(z) dA \gg \int_{A_c} B_z(z+6) dA$$

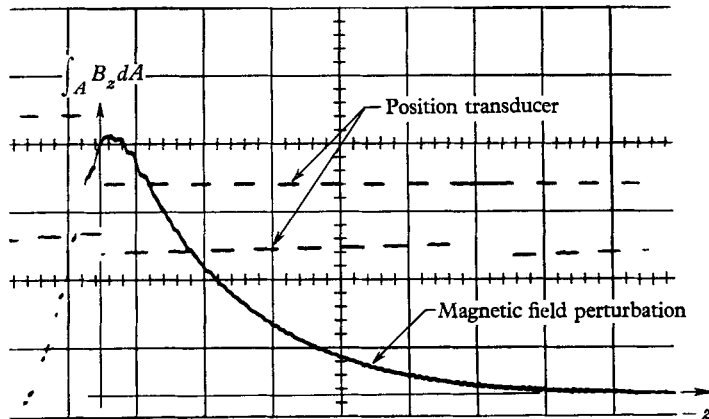


FIGURE 2. Typical recording of data.

for the region of interest; hence these data can be reduced to

$$\int_{A_c} B_z(z) dA.$$

A typical recording of the data is shown in figure 2 where the time increases from right to left. The upper trace is from a position transducer which locates the body with respect to the coil and together with the time scale of the trace gives the velocity of the body. The lower trace is the voltage from the coil and shows the typical axial variation of the magnetic field perturbation.

The experiments were performed for all four sets of coils and for the basic dimensionless parameters in the following ranges:

$$78,000 < Re < 400,000, \quad 0.012 < Rm < 0.061,$$

$$0.47 < \alpha < 18.2, \quad -1.90 < k < +0.024.$$

The ordinary Reynolds number, Re , is much greater than one, so the viscous effects should be unimportant except in the boundary layer. The magnetic Reynolds number, Rm , is much less than one so the magnetic field perturbations should also be much less than one. The Alfvén number, α , is varied from less

than one to greater than one and the magnetic Oseen number is both positive and negative so data was obtained both when a wake should exist upstream and when it should not.

3. Results of experiments

The results of the experiments are first presented in the form,

$$Rm^{-1} \int_A b_z dA = \text{fn}(z/D),$$

where b_z is the axial component of the dimensionless magnetic field perturbation and z/D is the axial distance from the nose of the body in dimensionless form (see figures 3 and 4). The first major result from this data is that Rm is the basic parameter in determining the perturbation near the body. Actually this result is expected, since the linearized equation with $Rm \ll 1$ for \mathbf{b} is

$$\text{curl } \mathbf{b} = -Rm(\mathbf{v} \times \mathbf{e}_z),$$

which suggests that $|\mathbf{b}| = O(Rm)$. Here $\mathbf{v} = \mathbf{V}/U$, \mathbf{e}_z is the unit vector in the z -direction, and $-B_0\mathbf{e}_z$ is the impressed magnetic field.

In § 1, it was pointed out that in the wake the perturbations ought to decay algebraically and outside the wake they ought to decay exponentially. For this configuration it can be shown that the perturbations in the wake ought to decay inversely as the distance from the body. However, the experimental data shows a most startling result for the region ahead of the body. It is found that the perturbations decay exponentially,

$$Rm^{-1} \int_A b_z dA \sim e^{+\lambda z/D},$$

for both cases, whether the theory predicts a wake or not. Moreover, λ is of a different order from the expected exponent outside the wake. In figure 3 two curves are shown for the case $k > 0$ when a wake should not exist forward of the body and two curves for $k < 0$ when a wake should exist forward of the body. In figure 4 four curves are shown for $k < 0$. Note that in these figures, where a semi-log scale is used, an exponential behaviour is indicated by a straight line. The reason for this apparent anomaly is that the walls of the tank and the solenoid surrounding the tank have a large effect on the flow. The theories are not incorrect; the forward wake exists and is shown by the experiments, but the wall effects dominate the behaviour of the decay of the perturbations for the range of values of the magnetic Oseen number, k , which were obtained in the experiments. The discussion of the wall effects will be given in § 5.

Figures 3 and 4 show that as k goes from positive to negative values and increases negatively, the rate of decay of the perturbations decreases. This change in the decay rate shows that a wake does exist in these experiments. Although the experiments do not check the infinite-fluid theories, the perturbations upstream still increase when the wake should exist. Since the whole flow has changed so much because of the walls, it may not be strictly proper to call the increased upstream disturbance a wake. However, this region still has con-

centrated currents and vorticity, so it will still be designated as a wake in this paper.

Figures 3 and 4 clearly show that Rm is one basic parameter of the flow, but it is not clear from these two figures whether α or k is the parameter which determines the decay rate of the perturbations. This question is completely

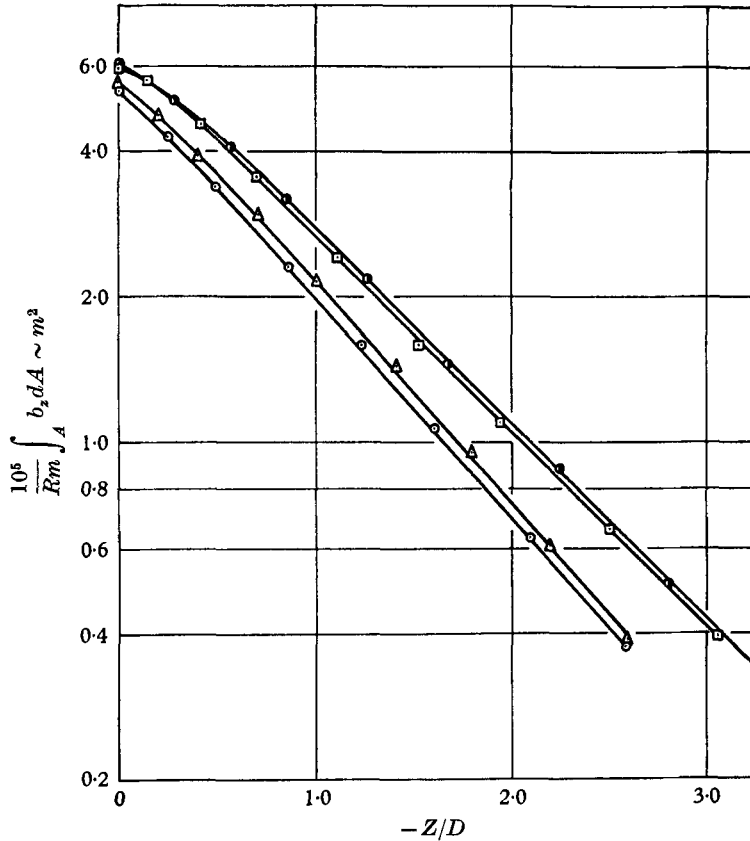


FIGURE 3. Axial-magnetic-field perturbation.

	D_c/D	Rm	α	k
○	1.54	0.0524	0.546	+0.0184
△	1.54	0.0425	0.674	+0.0116
□	1.54	0.0118	2.42	-0.0287
●	1.54	0.0119	4.96	-0.1400

resolved in figure 5 where data with different α and Rm , but the same k , are presented for each of the four sets of coils. The values of the dimensionless parameters are $\alpha \doteq 9.5$, $Rm \doteq 0.012$ and $\alpha \doteq 6.4$, $Rm \doteq 0.0265$ with $k \doteq -0.53$. There is a 50% change in α and 100% change in Rm and yet for each set of coils there is only one curve; thus k is the basic parameter for the strength of the wake. For k large and negative, a strong wake exists upstream of the body.

The equations for this problem show that a wake should exist not only in the magnetic field but also in the velocity field. Moreover, it was possible in the

experiments to make $\alpha^2 Rm > 1$. This is the parameter which governs the order of magnitude of the velocity perturbations due to the wake; the velocity perturbations are of order α^2 times the magnetic perturbations which are of order Rm (see § 5). The velocity wake should be quite similar in structure to the magnetic field wake, i.e. there should be an increased axial velocity defect forward of the body. With the increased axial velocity defect an increase in the radial velocity away from the body should occur, and near the body, especially when a strong wake is present, there should be a decrease in the radial velocity.

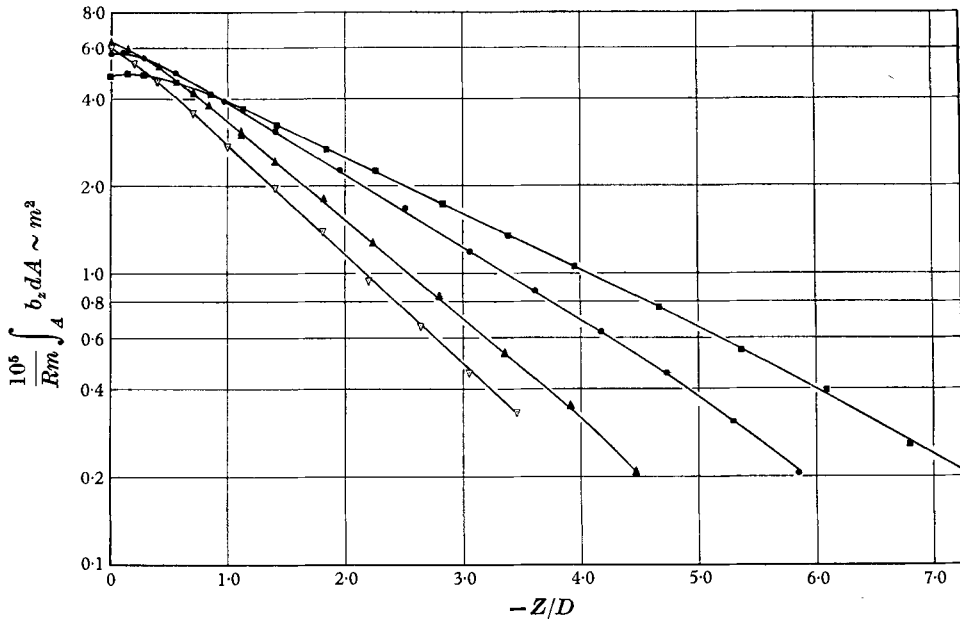


FIGURE 4. Axial-magnetic-field perturbation.

	D_c/D	Rm	α	k
▽	1.54	0.0423	3.99	-0.314
▲	1.54	0.0118	9.48	-0.527
●	1.54	0.0117	14.37	-1.206
■	1.54	0.0117	17.94	-1.88

A relationship between the magnetic field and the velocity field is given by the induction equation which can be simplified to $\text{curl } \mathbf{b} = Rm v_R \mathbf{e}_\theta$ for $Rm \ll 1$. Using this equation and the proposed description of the velocity wake given above, it is possible to predict the trends in the magnetic field perturbations and see if they agree with the experiments. This approach indicates that b_z and b_R should be larger for $k < 0$ than for $k > 0$ away from the body and conversely they should be smaller near the body. The effect of the decrease in b_z should appear further forward as the strength of the wake increases. In figures 3 and 4,

$$Rm^{-1} \int_A b_z dA$$

is shown as a function of z/D and a direct confirmation of the effect in b_z described above can be seen. Moreover

$$\frac{b_R}{Rm} \propto \frac{\partial}{\partial(z/D)} \left\{ Rm^{-1} \int_A b_z dA \right\}$$

so that b_R is obtained by taking the slopes of these curves and the effects predicted for b_R can also be seen.

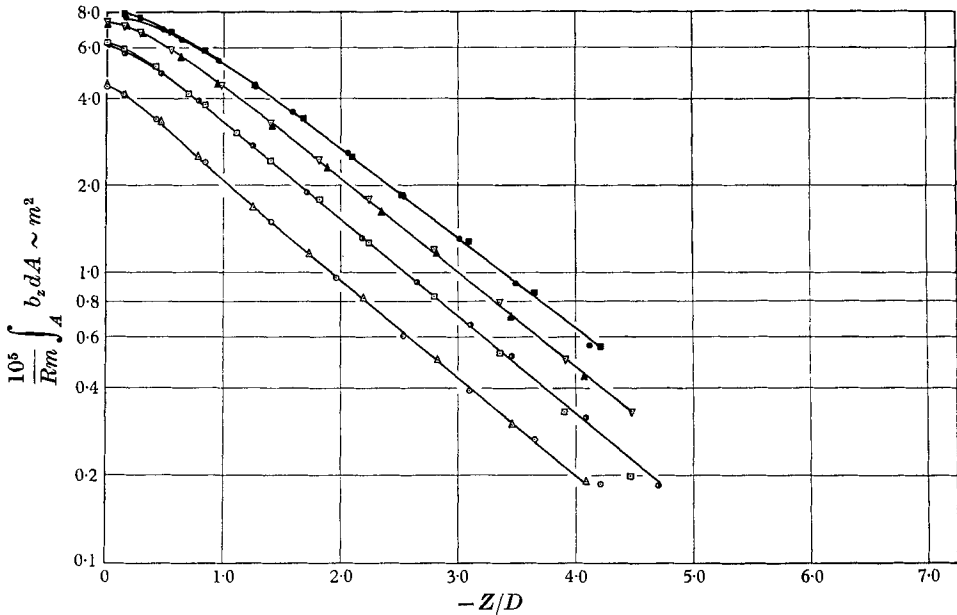


FIGURE 5. Effect of changing the Alfvén number and holding the magnetic Oseen number constant.

	D_c/D	Rm	α	k
○	1.16	0.0119	9.42	-0.524
△	1.16	0.0265	6.38	-0.526
□	1.54	0.0118	9.51	-0.528
●	1.54	0.0263	6.37	-0.524
▽	1.94	0.0119	9.48	-0.531
▲	1.94	0.0264	6.42	-0.530
■	2.34	0.0119	9.49	-0.529
●	2.34	0.0266	6.35	-0.522

It is also of interest to compare the radial distribution of b_z for $k > 0$ with that for $k < 0$. Figure 6 shows $b_z/Rm = \text{fn}(R/D, z/D)$, which is obtained by taking

$$\frac{b_z}{Rm} = (A_2 - A_1)^{-1} \left\{ Rm^{-1} \int_{A_2} b_z dA - Rm^{-1} \int_{A_1} b_z dA \right\}$$

for pairs of coils. This figure again shows the much slower decay of the perturbations in the axial direction for $k < 0$; but more important, there is very little difference between the radial distributions. This similarity in the radial distributions is another effect of the walls, i.e. the boundary conditions, on the problem.

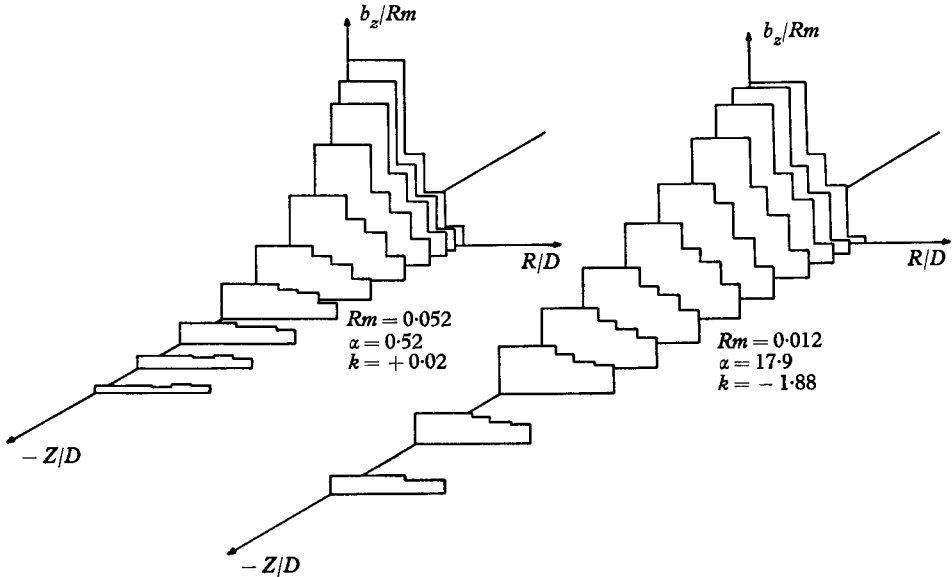


FIGURE 6. Radial and axial distribution of the perturbation of axial magnetic field.

4. Theoretical considerations

Although a great deal of theoretical work has been done for this problem, no solution has been presented for the semi-infinite Rankine body. Therefore it is useful for comparison with the experiments to work out an approximate solution in the infinite-fluid theory for some range covered by the experiments. However, this is only discussed briefly because the infinite-fluid theory turns out to be inadequate.

It is assumed that $Rm \ll 1$, $|\mathbf{b}| \ll 1$ and $|k| \ll 1$. The first two assumptions are satisfied by all the data and the third assumption is valid for some of the experiments. Then for these assumptions, to first order, the velocity field is the potential field, and the magnetic field is the uniform applied field, $-B_0 \mathbf{e}_z$. From this information it is possible to calculate the first perturbation on the magnetic field. The equations required are

$$\text{curl } \mathbf{b} = -Rm(\mathbf{v} \times \mathbf{e}_z), \quad \text{div } \mathbf{b} = 0.$$

Substituting the appropriate expression for \mathbf{v} and introducing the stream function Ψ for the magnetic field \mathbf{b} , it is found that

$$r^2 \frac{\partial^2 \Psi}{\partial r^2} - \cot \theta \frac{\partial \Psi}{\partial \theta} + \frac{\partial^2 \Psi}{\partial \theta^2} = -\frac{Rm}{16} r \sin^2 \theta,$$

$$b_r = \frac{1}{r^2 \sin \theta} \frac{\partial \Psi}{\partial \theta}, \quad b_\theta = -\frac{1}{r \sin \theta} \frac{\partial \Psi}{\partial r},$$

where (r, θ) are spherical polar co-ordinates. The particular solution of this equation which satisfies the boundary conditions at infinity and which is the dominant contribution for large r is the Stokeslet: $\Psi = \frac{1}{32} Rm r \sin^2 \theta$. The term Stokeslet is commonly used to denote the particular form of the stream function

which is obtained in the solution for axisymmetric bodies in ordinary Stokes flow. This solution is not complete since it does not satisfy the boundary conditions at the body. The complete solution would require, in addition, potential solutions inside and outside the body to satisfy the boundary conditions that

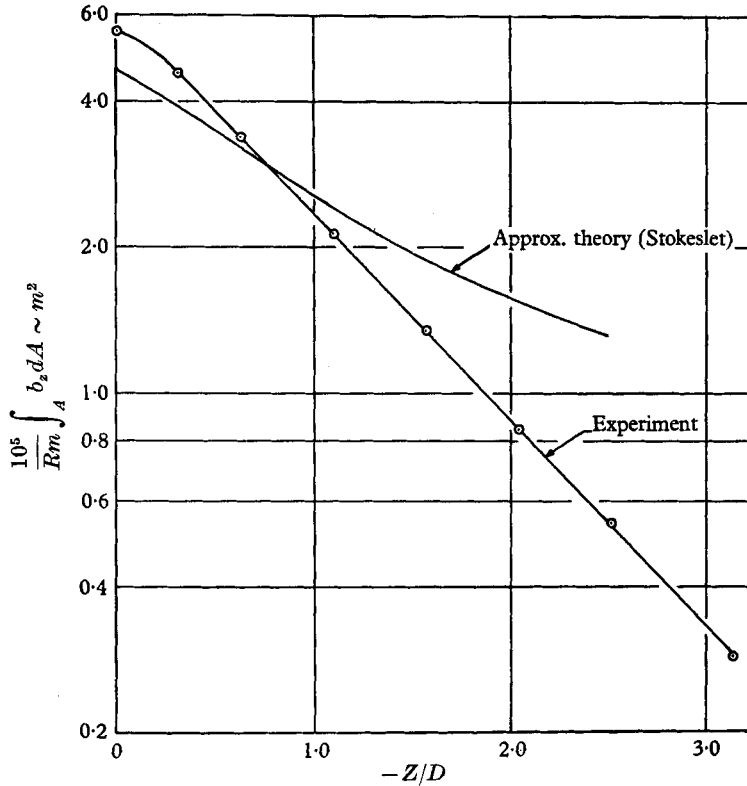


FIGURE 7. Comparison of infinite-fluid theory with experiments.
 $Rm = 0.027$, $\alpha = 1.06$, $k = -0.0018$, $D_c/D = 1.54$.

the magnetic field be continuous across the boundary of the body. However, this particular solution contains the major contribution at large distances from the body.

Away from the body this solution gives $b_r \sim 1/r$. Thus, the expected decay is obtained but the wake effect has been lost. Upon closer examination of the equations it is found that the equation for the electric current density, \mathbf{J} , in this approximation is $\nabla^2 \mathbf{J} = 0$, whereas a better approximation is $(\nabla^2 - 2k \partial/\partial z) \mathbf{J} = 0$, (see Appendix). Thus it is seen that the solution obtained is a Stokes approximation, and one should go back and put in one convection term to get the wake effect. By analogy with Oseen's solution for ordinary fluid dynamics, this changes the Stokeslet solution to the form of

$$b_r \sim (1/r) \exp\{-|k|r + kz\}.$$

To compare this approximate solution with the experiments, a case is chosen with $k = -0.0018$ so that the effect of the exponential factor is negligible in the

range $-4 < z/D < 0$. This comparison is shown in figure 7. The Stokeslet checks nicely for order of magnitude but the rate of decay is rapidly divergent; for the Stokeslet $b_z \sim (z/D)^{-1}$ and for the experiments $b_z \sim e^{+\lambda z/D}$ where $\lambda \doteq 1$. For all the experiments, $0.4 < \lambda < 1.4$, so that this theory cannot explain the exponential decays which were observed. The disagreement is particularly striking for the cases when $k < 0$, since here the theory predicts algebraic decay ahead of the body.

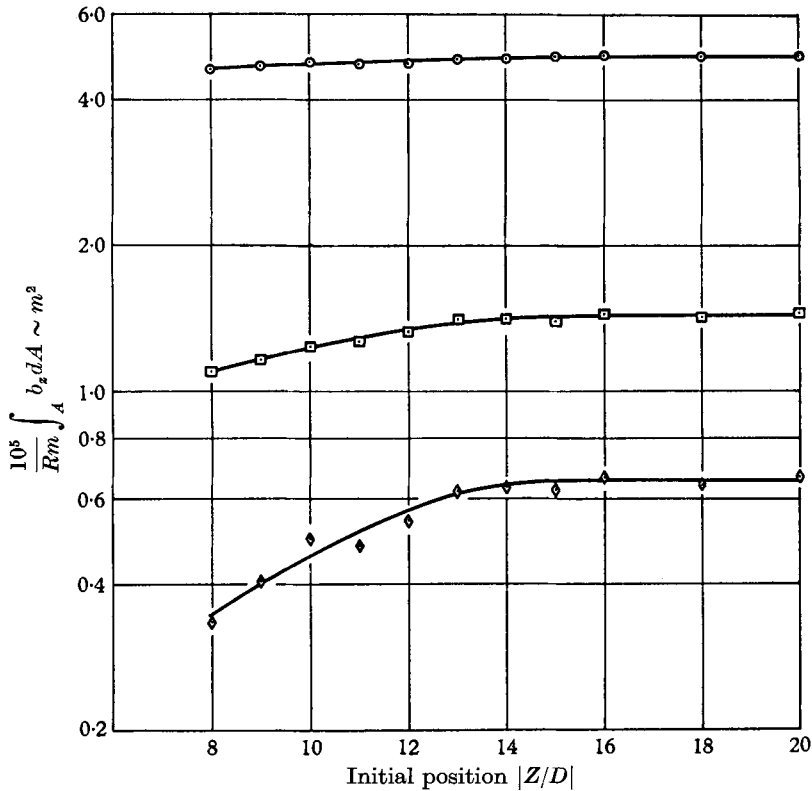


FIGURE 8. Effect of initial position on the magnetic-field perturbations.

	Rm	α	k	Z/D
○	0.0118	14.3	-1.20	-1.5
□	0.0118	14.3	-1.20	-4.0
◇	0.0118	14.3	-1.20	-5.5

At this point it is well to consider the question as to whether or not a steady flow was attained in the experiments. Since the body starts moving at a finite distance from the pick-up coils, it is possible that the measurements were made before the steady flow became established. In order to check this effect, experiments were performed in which the starting distance was varied from 8 to 20 body diameters. The results of these experiments are shown in figures 8 and 9. In figure 8 the perturbation at a given distance from the body remains constant for initial positions greater than 15 and decreases for initial positions less than 15. In figure 9 the perturbation is plotted as a function of the distance from the

body for three initial positions. The two curves for initial positions of 16 and 20 are identical and the third curve for an initial position of 8 shows how the starting affects the data. Since all the normal data were taken at an initial position of 20, it is concluded that the flow was established, and this is not an effect in the difference between the infinite-fluid theory and the experiments.

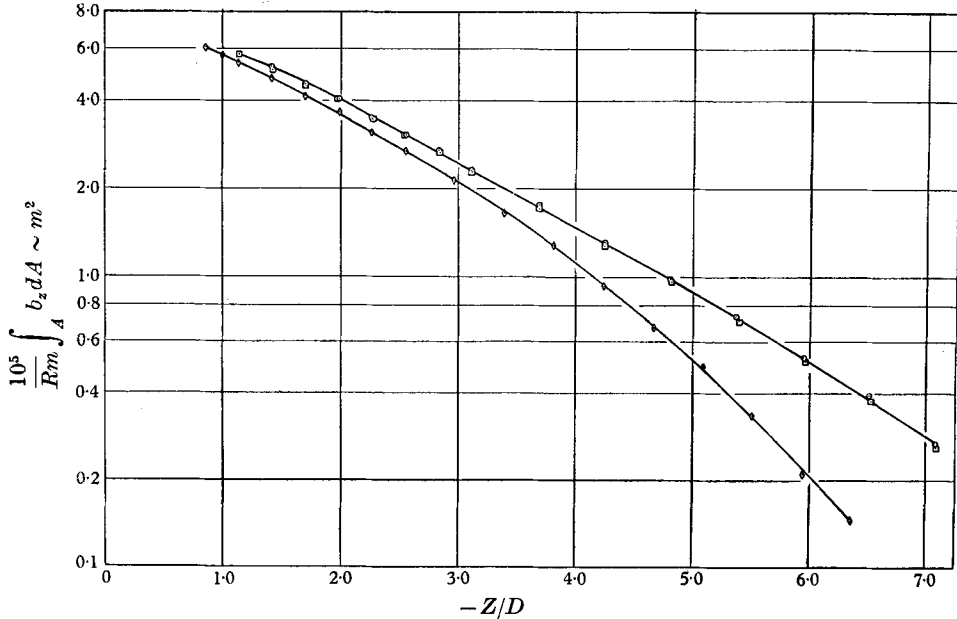


FIGURE 9. Effect of initial position on the axial distribution of the magnetic-field perturbation.

	Rm	α	k	Initial position $ Z/D $
○	0.0118	14.3	-1.20	20
□	0.0118	14.3	-1.20	16
◇	0.0118	14.3	-1.20	8

5. Effect of the boundary conditions

Since the experiments were correct in that the flow was steady and the theory, though only approximate, should at least give the correct decay in the far field, there is only one possibility left to consider. The theory and the experiments are for different conditions. The difference of the conditions is that the theory is for an infinite medium while the experiments were performed in a tube of fluid which is surrounded by a large copper solenoid.

The change in the far-field behaviour of the perturbations must be due to the fluid-dynamic boundary conditions at the wall of the tube, the electromagnetic boundary conditions due to the solenoid, or both. The fluid-dynamic boundary condition is obvious, i.e. there can be no flow normal to the wall. The electromagnetic boundary condition due to the solenoid is not so clearly defined. However, in general, a mass of metal tends to resist a change in flux in the metal. If the conductivity of the metal becomes infinite, then surface currents are set

up which eliminate the field from the metal and impose the boundary condition that at the surface there can be no normal component of the magnetic field.

To unravel the effect of the solenoid it is first assumed that copper of the solenoid is not cut by insulating surfaces so that the simple concept of field diffusion distance is significant. If the copper were a solid mass then the diffusion length for these experiments would be given by

$$L_D = O\{(D/\sigma\mu U)^{\frac{1}{2}}\} \leq \frac{1}{2} \text{ in.}$$

Thus it appears that the field may be trapped by the solenoid. This model was suggested by Dr G. B. Whitham. Now recourse to a simple experiment can prove this effect. In order to remove the magneto-fluid-dynamic effects the experiment chosen was that of a current loop running through the solenoid in the absence of the mercury and in the absence of a uniform magnetic field. The field generated by the current loop was measured with the pick-up coils.

If the solenoid had no effect on the distribution of the magnetic field produced by the current loop then the solution would be that for an infinite medium as given for example by Smythe (1950)

$$\int_{A_c} B_z dA = 2\mu I \sqrt{(aR)} \frac{1}{k} \{(1 - \frac{1}{2}k^2) K(k) - E(k)\},$$

where $k^2 = 4aR/\{(a+R)^2 + z^2\}$, $K(k)$ and $E(k)$ are the complete elliptic integrals of the first and second kinds and a is the radius of the current loop. This solution gives

$$\int_{A_c} B_z dA \sim z^{-3}.$$

If the solenoid acts as an infinitely conducting wall then the solution should be that for a current loop in an infinitely conducting tube,

$$\int_{A_c} B_z dA = 2\pi \sum_{n=1}^{\infty} C_n R J_1\left(j_n \frac{R}{b}\right) \exp(\pm j_n z/b),$$

where $J_1(x)$ is the Bessel function, the j_n 's are the zeros of this Bessel function and b is the radius of the tube. For large axial distances $|z| \gg b$ this solution gives $\int B_z dA \sim \exp(\pm j_1 z/b)$. This solution produces currents on the inner surface of the tube which are a symmetric function of the axial coordinate z . These surface currents, J_θ , are given by

$$J_\theta = \sum_{n=1}^{\infty} \frac{C_n j_n}{\mu b} J_0(j_n) \exp(\pm j_n z/b).$$

The results of these experiments are presented in figure 10 along with the calculated results for an infinite medium and for the current loop in an infinitely conducting tube. The experiments exhibit an exponential decay which is the same as for the infinitely conducting tube solution with $b = 0.3$ in., the inner radius of the solenoid. Although the experiments give values somewhat larger than the calculated values there can be no doubt that the solenoid acts approximately as an infinitely-conducting tube. Although it is not obvious that non-uniform currents, $I = f(z)$, should flow in the solenoid for the large characteristic

times in these experiments, $\tau = O(D/U) \leq 0.06$ sec, the experiments with the current loop are sufficient proof that they must.

It is interesting to notice that the exponential decay obtained in the experiments with the current loop, $j_1/b = 1.28$, is of the same order of magnitude as that obtained in the magneto-fluid-dynamic experiments, $\lambda = O(1)$. Now using

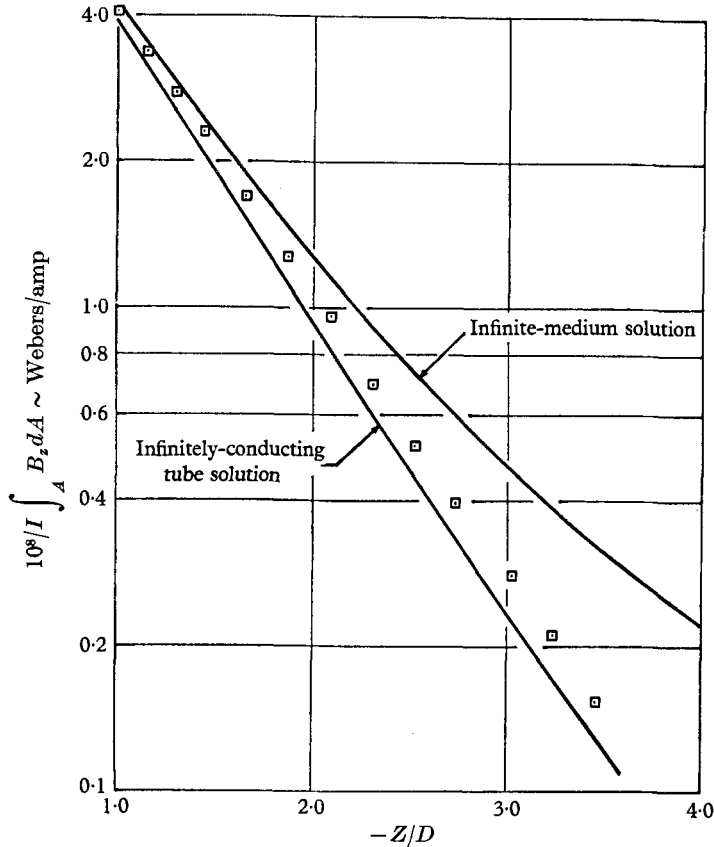


FIGURE 10. Comparison of calculated infinite-medium and infinitely-conducting-wall solutions with the experiments performed with a 0.612 in.-diameter current loop. \square , Experiments $D_c/D = 2.34$.

the boundary conditions that at the wall there can be no normal component of the velocity or the magnetic field, the magneto-fluid-dynamic problem can be attacked. The equations for this case are the induction equation and the momentum equation. If these equations are linearized and put in terms of the fluid-dynamic stream function, η , and the magnetic stream function Ψ , they become (see Appendix)

$$D^2\Psi = Rm\left(\frac{\partial\Psi}{\partial z} + \frac{\partial\eta}{\partial z}\right), \quad D^2(\eta + \alpha^2\Psi) = 0,$$

where

$$D^2 = \frac{\partial^2}{\partial z^2} + \frac{\partial^2}{\partial R^2} - \frac{1}{R} \frac{\partial}{\partial R}$$

in cylindrical co-ordinates. Then the equations can be uncoupled by defining two new functions such that

$$\Psi = \Phi + \chi, \quad \eta = -\Phi - \alpha^2 \chi,$$

and the equations become

$$D^2 \Phi = 0 \quad \text{and} \quad \left(D^2 - 2k \frac{\partial}{\partial z} \right) \chi = 0.$$

The boundary conditions on Ψ and η are

$$\Psi = 0 \quad \text{and} \quad \eta = 0 \quad \text{on} \quad R = b,$$

so the boundary conditions on Φ and χ are also

$$\Phi = 0 \quad \text{and} \quad \chi = 0 \quad \text{on} \quad R = b.$$

The eigensolutions for these equations can be found for the cylindrical geometry and from these modes the possible decay rates can be found without actually solving the boundary-value problem for the particular body used.

The eigensolutions for Φ are

$$\Phi_n = RJ_1 \left(j_n \frac{R}{b} \right) \exp(\pm j_n z/b), \quad + \text{ for } z < 0, \quad - \text{ for } z > 0,$$

and the eigensolutions for χ are

$$\chi_n = RJ_1 \left(j_n \frac{R}{b} \right) \exp \begin{cases} \lambda_n z & z < 0, \\ -\mu_n z & z > 0, \end{cases}$$

where $\mu_n = -k + (k^2 + j_n^2/b^2)^{1/2}$ and $\lambda_n = k + (k^2 + j_n^2/b^2)^{1/2}$; the variation of μ_n and λ_n with k is sketched in figure 11. Thus, from the eigensolutions of the equations it is found that the decay rate varies with k . In order to check this effect with the experiments, λ_1 is plotted against k , taking $b = 3.0$ in., and compared with the experimental decay rates from the data for one set of coils. This comparison is shown in figure 12. This approximation not only gives the same trend as the experiments but also differs by a maximum of only 30% over the range of the experiments.

Thus it has been shown that wall effects are extremely important in investigating this area in magneto-fluid dynamics. In this case the effect of the walls is such that it changes the whole character of the flow from an algebraic decay of the perturbations to exponential decay. This case is analogous to the classical fluid-dynamic problem where for the same body to wall diameter ratio the wall effects at low Reynolds number are much larger than for high Reynolds number flow. In this magneto-fluid-dynamic case the appropriate dimensionless number is the magnetic Oseen number. In the limit $k^2 \gg j_1^2/b^2$, which can be attained either by making k^2 large or by letting $b^2 \rightarrow \infty$,

$$\mu_1 \rightarrow -k + |k| \quad \text{and} \quad \lambda_1 \rightarrow k + |k|.$$

Then for this limit, one should achieve the infinite fluid solution of an algebraic decay within the wakes and an exponential decay with a rate of $2k$ outside the wakes. For the experiments this limit is not attained so the wall effects are important.

A final interesting point arising from the experiments is that a direct measure of the perturbation magnetic stream function, Ψ , is obtained (see § 2). This measurement makes it possible to plot the perturbation which is generated. It

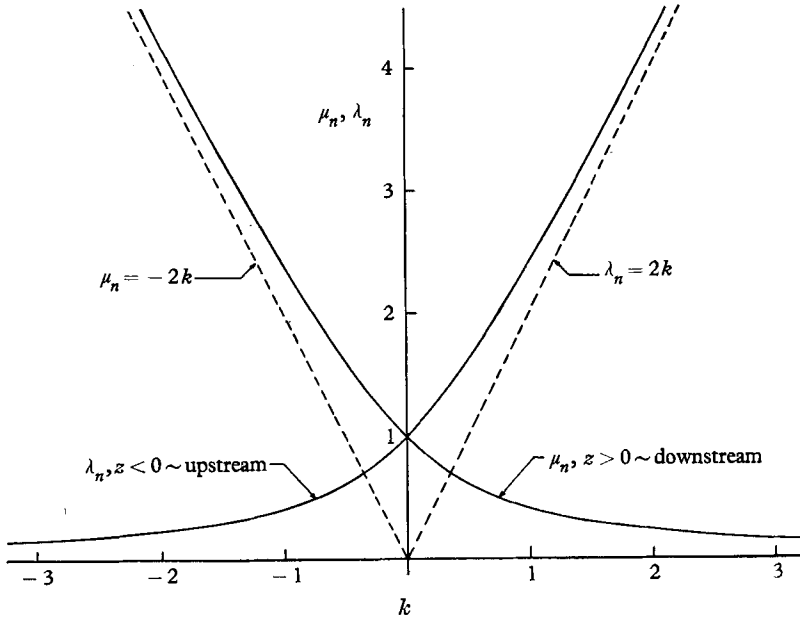


FIGURE 11. Decay rates predicted by eigensolutions.

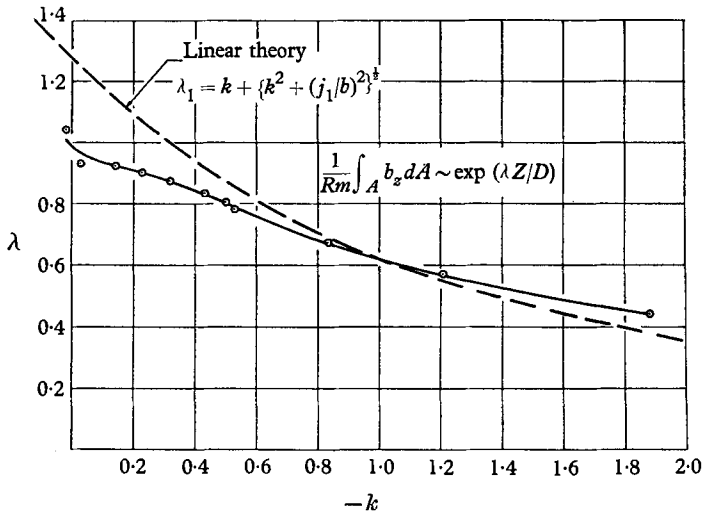


FIGURE 12. Comparison of experimental and theoretical decay rates.

should be possible from these data to see that $\Psi \rightarrow 0$ at $R = b$. In figure 13, Ψ is plotted for $k > 0$ and $k < 0$ so that the effect of the wake is again observed but also one notices that the field lines in the figure are starting to reverse and form closed curves so that the effect of the walls is again demonstrated.

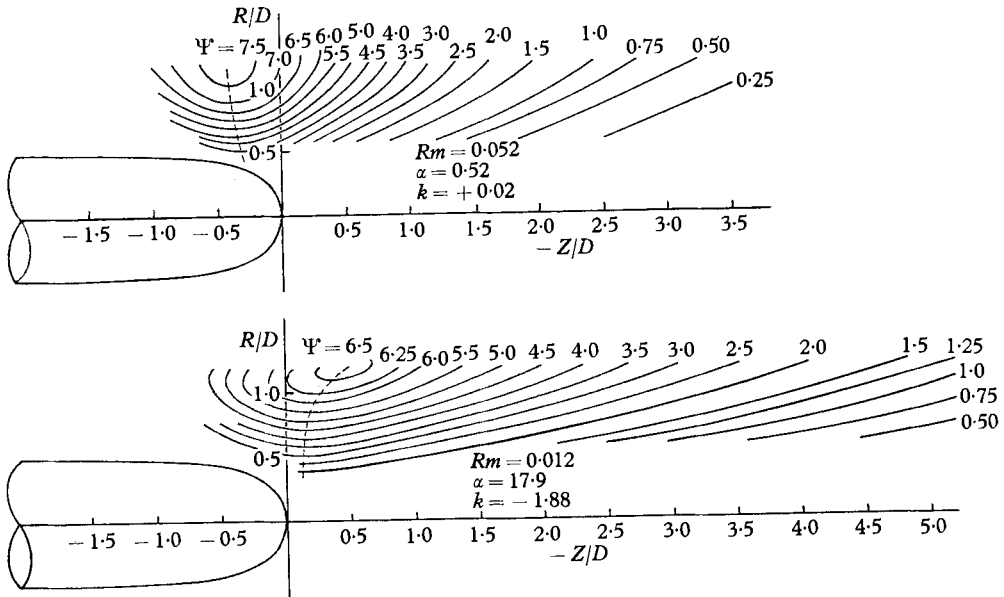


FIGURE 13. Perturbation magnetic stream function.

6. Conclusions

Experiments have been performed on a semi-infinite Rankine body in a uniform magnetic field which is parallel to the direction of motion and the magnetic field perturbations forward of the body have been measured. As a result of these measurements it has been shown that the magnetic Reynolds number determines the order of magnitude of the disturbance. A wake upstream of the body has been observed and its effects are determined by the magnetic Oseen number. Finally it has been shown that the disagreement between the infinite fluid theories and the experiments is due to wall effects, and by a simple theoretical approach results have been found which give an estimate of the ranges of the parameters in which the wall effects should be important.

The author would like to express his sincere gratitude to Dr H. W. Liepmann for suggesting this problem and for his many helpful suggestions and encouragements. Thanks are also due to Dr G. B. Whitham for his help and actual contributions to the theoretical part of this paper and to Dr D. P. Hoult for designing and building the mercury tow tank and for many helpful discussions.

This research was supported by the Office of Naval Research under contract number N-onr-220(21).

REFERENCES

- CHESTER, W. 1957 *J. Fluid Mech.* **3**, 304.
 GOULDINE, M. 1961 *J. Fluid Mech.* **10**, 439.
 GREENSPAN, H. P. & CARRIER, G. F. 1959 *J. Fluid Mech.* **6**, 77.
 LARY, E. C. 1962 *J. Fluid Mech.* **12**, 209.

LIEPMANN, H. W., HOULT, D. P. & AHLSTROM, H. G. 1962 *Miszellaneen der Angewandten Mechanik*, p. 175. Berlin: Akademie-Verlag.

SMYTHE, W. R. 1950 *Static and Dynamic Electricity*, 2nd ed., p. 271. New York: McGraw-Hill.

STEWARTSON, K. 1960 *J. Fluid Mech.* **8**, 82.

TAMADA, K. 1961 *AFOSR*, no. 1087.

VAN BLERKOM, R. 1960 *J. Fluid Mech.* **8**, 432.

Appendix

The linearized equations of magneto-fluid dynamics for the problem discussed in this paper are

$$\operatorname{div} \mathbf{v} = 0, \quad (1)$$

$$\frac{\partial}{\partial z} \mathbf{v} = -\operatorname{grad}(p - b_z) - \alpha^2 \frac{\partial}{\partial z} \mathbf{b} + \frac{1}{Re} \nabla^2 \mathbf{v}, \quad (2)$$

$$\operatorname{curl} \mathbf{b} = \mathbf{J}, \quad (3)$$

$$\operatorname{div} \mathbf{b} = 0, \quad (4)$$

and

$$\mathbf{J} = Rm(b_R + v_R) \mathbf{e}_\theta. \quad (5)$$

Eliminating \mathbf{v} , \mathbf{b} and p and introducing $\boldsymbol{\omega} = \operatorname{curl} \mathbf{v}$, one obtains the following equations for $\boldsymbol{\omega}$ and \mathbf{J} :

$$\nabla^2 \mathbf{J} = Rm \left(\frac{\partial \mathbf{J}}{\partial z} + \frac{\partial \boldsymbol{\omega}}{\partial z} \right) \quad (6)$$

and

$$\alpha^2 \frac{\partial \mathbf{J}}{\partial z} + \frac{\partial \boldsymbol{\omega}}{\partial z} = \frac{1}{Re} \nabla^2 \boldsymbol{\omega}. \quad (7)$$

In the limit $Re \rightarrow \infty$ equation (7) becomes

$$\boldsymbol{\omega} = -\alpha^2 \mathbf{J}, \quad (8)$$

provided $\boldsymbol{\omega}$ and $\mathbf{J} \rightarrow 0$ for $|z| \rightarrow \infty$. This boundary condition is applicable for the upstream direction as long as Rm is finite and not too large, but in the downstream direction there is serious doubt as to the applicability of this boundary condition. However, this paper is concerned with the upstream direction and $Rm \ll 1$ so that equation (8) can be used. Then from equations (6) and (8), Oseen equations for the current and vorticity are obtained,

$$\left(\nabla^2 - 2k \frac{\partial}{\partial z} \right) \mathbf{J}, \boldsymbol{\omega} = 0. \quad (9)$$

Another form of the equations is used in which stream functions, η for the velocity field and Ψ for the magnetic field, are introduced, where η and Ψ are defined by

$$v_z, b_z = \frac{1}{R} \frac{\partial}{\partial R} (\eta, \Psi) \quad \text{and} \quad v_R, b_R = -\frac{1}{R} \frac{\partial}{\partial z} (\eta, \Psi). \quad (10)$$

Then substituting equation (10) into equations (5) and (8), the momentum and induction equations are obtained in terms of η and Ψ ,

$$D^2(\eta + \alpha^2 \Psi) = 0, \quad (11)$$

and

$$D^2 \Psi = Rm \left(\frac{\partial \Psi}{\partial z} + \frac{\partial \eta}{\partial z} \right), \quad (12)$$

where

$$D^2 = \frac{\partial^2}{\partial z^2} + \frac{\partial^2}{\partial R^2} - \frac{1}{R} \frac{\partial}{\partial R}$$

in cylindrical co-ordinates.